Journal of Guidance, Control, and Dynamics
Vol. 39, No. 9, September 2016

Underactuated Spacecraft Switching Law for Two Reaction Wheels and Constant Angular Momentum

Christopher D. Petersen*
University of Michigan, Ann Arbor, Michigan, 48109
Frederick Leve†
U.S. Air Force Research Laboratory, Kirtland Air Force Base, Albuquerque, New Mexico 87117
and
Ilya Kolmanovsky‡
University of Michigan, Ann Arbor, Michigan, 48109

DOI: 10.2514/1.G001680

This paper develops a switching feedback controller for the attitude of an underactuated spacecraft that exploits two internal control torques provided by reaction wheels. The problem is challenging; for example, even in the zero total angular momentum case, no smooth or even continuous time-invariant feedback law for stabilizing a desired orientation exists. The method introduced here exploits the separation of the system states into inner-loop base variables and outer-loop fiber variables. The base variables track periodic reference trajectories, the amplitude of which is governed by parameters that are adjusted to induce an appropriate change in the fiber variables. Under suitable assumptions on the total angular momentum, this controller stabilizes an equilibrium that corresponds to a desired inertially fixed orientation. If the desired attitude violates the assumption on angular momentum, then controlled oscillations in a neighborhood around the target orientation are induced by the switching controller. The control scheme is based on several approximations and is designed for relatively small maneuvers close to the desired attitude in a vicinity which may be achieved by thruster-based control schemes. Simulation results demonstrate that the switching feedback law provides good performance in controlling the attitude of an underactuated spacecraft.

Nomenclature

A	=	dynamics matrix for the base variables
B	=	input matrix for the base variables
$\mathcal{B}$	=	spacecraft bus fixed frame
$\hat{b}_1, \hat{b}_2, \hat{b}_3$	=	orthogonal unit vectors of $\mathcal{B}$
e_θ	=	error between θ and $\bar{\theta}$
e_ϕ	=	error between ϕ and $\bar{\phi}$
e_ψ	=	error between ψ and $\bar{\psi}$
G	=	map from (α_1, α_2) to $\Delta\psi$
G_a	=	map from (α_1, α_2) to $\Delta_a\psi$
G_{a,h_3}	=	map from (α_1, α_2) to $\Delta_{a,h_3}\psi$
$G_{a,\delta\alpha_{2,e}}$	=	map from $\delta\alpha_{2,e}$ to $\Delta_{a,h_3}\psi$
$\boldsymbol{H}$	=	physical total angular momentum vector
H	=	mathematical vector corresponding to $\boldsymbol{H}$ expressed in $\mathcal{I}$
h_1, h_2, h_3	=	components of H
$\mathcal{I}$	=	inertial frame corresponding to the desired attitude
J_1, J_2, J_3	=	spacecraft bus principal moments of inertia
$\bar{J}_0$	=	inertia matrix of spacecraft bus relative to the center of mass of the spacecraft assembly and expressed in $\mathcal{B}$
$\bar{J}_{w1}, \bar{J}_{w2}$	=	inertia matrices of reaction wheels 1 and 2 relative to the center of mass of the spacecraft assembly and expressed in $\mathcal{B}$
J_{s1}, J_{s2}	=	inertias of reaction wheels 1 and 2 about their spin axes
$\bar{J}$	=	total inertia matrix
$j_{l,m}$	=	(l, m)th component of matrix $\bar{J}$; in which l and m are each equal to 1, 2, 3
k	=	cycle number
$k_{l,m}$	=	feedback linearization parameters; in which l and m are each equal to 1, 2
$\boldsymbol{M}_{\text{ext}}$	=	physical external moment vector
n	=	base dynamic excitation frequency
$\mathcal{O}_{\mathcal{B}/\mathcal{I}}$	=	orientation matrix of $\mathcal{B}$ relative to $\mathcal{I}$
T	=	time period of one base dynamic excitation cycle
u	=	mathematical vector of control inputs corresponding to the accelerations of reaction wheels
v	=	control input to the linearized base dynamics
v_{fb}	=	mathematical vector of feedback linearization parameters
v_1, v_2	=	Components of v
W	=	matrix of reaction wheel spin axes
$\bar{W}$	=	reaction wheel influence matrix
$\hat{w}_1, \hat{w}_2$	=	physical unit vectors of reaction wheel spin axes
x	=	mathematical vector of base variables ϕ, θ, ω_1, and ω_2
$\bar{x}$	=	mathematical vector of steady-state base variable motions $\bar{\phi}$, $\bar{\theta}$, and $\bar{\omega}_1$, $\bar{\omega}_2$
α_1, α_2	=	amplitude of base dynamic excitation
$\alpha_{2,e}$	=	value of α_2 to counteract drift when $h_3 \neq 0$
β_m	=	coefficients of steady-state base variable amplitudes; in which m is equal to 1, 2, 3, 4
Γ_m	=	coefficients of G_a; in which m is equal to 1, 2, 3
$\bar{\Gamma}_0, \bar{\Gamma}_{l,m}$	=	coefficients of G_{a,h_3}; in which l is equal to 1, 2 and m is equal to 1, 2, 3, 4
γ_m	=	parameters of steady-state base variable phase shift; in which m is equal to 1, 2, 3, 4
$\bar{\gamma}_1, \bar{\gamma}_4$	=	values of γ_1 and γ_4 for large n
$\Delta\psi$	=	change in ψ over one cycle of length T induced by steady-state base variable motions
$\Delta_a\psi$	=	approximation of $\Delta\psi$ assuming small angles and $h_3 = 0$
$\Delta_{a,h_3}\psi$	=	approximation of $\Delta\psi$ assuming small angles and $h_3 \neq 0$
δ_1, δ_2	=	phase shift of base dynamic excitation

Received 5 September 2015; revision received 4 April 2016; accepted for publication 15 May 2016; published online 13 July 2016.

*Graduate Student, Department of Aerospace Engineering. Member AIAA.
†Research Aerospace Engineer.
‡Professor, Department of Aerospace Engineering. Member AIAA.

$\delta\alpha_{2,e}$	=	deviation of α_2 from $\alpha_{2,e}$
ϵ	=	control parameter for Algorithm (1)
ϵ_e	=	value of ϵ to counteract drift when $h_3 \neq 0$
$\Lambda_a, \Lambda_b, \Lambda_c$	=	coefficients for the mapping from (α_2, ϵ) to $\Delta_{a,h_3}\psi$
$\bar{\Lambda}_1, \bar{\Lambda}_2$	=	coefficients of $G_{a,\delta\alpha_{2,e}}$
μ_1	=	parameter for decreasing the amplitude of base variable excitation
μ_2	=	"dither" parameter to counteract error in approximation
ν_1, ν_2	=	speeds (spin rates) of reaction wheels 1 and 2, respectively
ν	=	mathematical vector of reaction wheels speeds
Θ	=	mathematical vector of Euler angles
$\Phi(t, t_0)$	=	state transition matrix from t_0 to t
Ξ	=	matrix representation of G_a
ξ_m, $m = 1, 2, 3$	=	initialization values for switching algorithms
ψ, θ, ϕ	=	3-2-1 Euler angles yaw, pitch, and roll
$\bar{\psi}, \bar{\theta}, \bar{\phi}$	=	steady-state motions of ψ, θ, and ϕ
$\dot{\bar{\psi}}$	=	average rate of change of ψ over one steady-state cycle
$\boldsymbol{\omega}$	=	physical angular velocity vector
ω	=	mathematical vector $\boldsymbol{\omega}$ expressed in $\mathcal{B}$
$\omega_1, \omega_2, \omega_3$	=	components of $\bar{\omega}$
$\bar{\omega}_1, \bar{\omega}_2$	=	steady-state values of ω_1 and ω_2

Subscripts

$(*)_c$	=	cosine of $*$
$(*)_s$	=	sine of $*$
$(*)_{\sec}$	=	secant of $*$
$*^k$	=	value of $*$ at time kT

I. Introduction

INTERNAL torque actuators, such as reaction wheels (RWs), can execute high-precision pointing missions that external moment actuation with thruster pairs cannot achieve. However, unlike thruster pairs, internal actuation is constrained by the total angular momentum of the spacecraft. This constraint becomes more prevalent when there are two or fewer RWs because the dynamics of the spacecraft become inaccessible [1], which can severely impede achieving mission objectives. There are numerous examples of recent spacecraft which, due to several failures, became underactuated. The Kepler telescope [2], FUSE [3] and Hayabusa [4] all suffered multiple RW failures within nominal RW design life that compromised their respective missions. Hence, there is a growing interest in developing methods for underactuated spacecraft attitude control with internal torques.

Because the dynamics of the spacecraft are inaccessible with two or fewer RWs, the attitude motions that can be achieved are restricted. In the case of zero total angular momentum, the spacecraft dynamics are small-time locally controllable and arbitrary rest-to-rest orientation maneuvers are possible [5], but the desired equilibrium orientation cannot be stabilized by any smooth or continuous feedback law due to Brockett's condition [5–8]. Time-periodic laws can achieve attitude stabilization with two RWs, but exponential convergence rates cannot be achieved if the control law is smooth [9].

Much of the literature pertaining to the control of a spacecraft with two RWs assumes that the total angular momentum is zero. For instance, in [5], two methods are proposed for attitude stabilization of an underactuated spacecraft under this assumption. The first is a finite-time discontinuous controller that induces a sequence of rotations, while the second exploits a diffeomorphic transformation that converts the equations of motion to a simpler form for controller design. Ge and Chen [10] solve an open-loop trajectory optimization problem with a genetic algorithm for a spacecraft with zero angular momentum. In [11], a singular quaternion feedback approach is implemented to stabilize the attitude of a spacecraft with no momentum bias and uses a saturation function to avoid singularities. The authors of [12–14] develop discontinuous control laws based on Lyapunov theory that are able to stabilize to the desired orientation in the zero total angular momentum case, while having bounded oscillations with momentum bias present. Techniques from nonholonomic control literature, in particular based on averaging [9,15], have also been applied to underactuated spacecraft with zero total angular momentum (e.g., [16–18]). Yamada et al. [18] exploits related ideas to this work; however, the approach of this paper is different in that it relies on a switching scheme, can be applied to general spacecraft configurations, and can handle nonzero angular momentum.

We note that the assumption of zero total angular momentum is restrictive. First, zero total angular momentum is hard to achieve in the space environment. Second, for an underactuated spacecraft, the RWs must spin down to zero speed for inertial pointing. As the RWs spin down, stiction and Coulomb friction take effect, reducing accuracy of the RW control and lifetime of the rotor bearings.

The case of nonzero total angular momentum is less studied. Boyer and Alamir [19] considers a subspace of feasible attitudes defined by the law of angular momentum conservation and defines a procedure for constructing an open-loop control. A spin-axis stabilization is performed about the uncontrollable axis of a spacecraft with nonzero total angular momentum in [20], but the topic of inertial pointing is not discussed. Katsuyama et al. [21] discuss the topic of control of an underactuated spacecraft with two RWs and initial nonzero angular momentum, but the proposed control law can send the spacecraft into an uncontrolled rotation for some initial conditions. Solar radiation pressure torques are taken into consideration in [22,23]; and, under suitable asymmetry conditions, the underactuated spacecraft dynamics become linearly controllable. Conventional linear quadratic controllers can then be used to stabilize a spacecraft with two RWs, but the maneuvers typically take time because the solar radiation pressure torques are relatively small.

This paper describes a new attitude control scheme for an underactuated spacecraft with two RWs when maneuvers being performed are small and close to the desired pointing configuration. The approach uses the switching feedback stabilization techniques of [24,25], which exploit the decomposition of the system variables into base variables and fiber variables. The base variables are stabilized to periodic motions with feedback, and the parameters of these periodic motions are adjusted at discrete time instants to induce a change in the fiber variables toward the desired equilibrium. For a spacecraft actuated with two RWs, the Euler angles and the angular velocities corresponding to the two actuated axes are treated as base variables while the Euler angle corresponding to the uncontrolled axis is treated as the fiber variable. There are several advantages to this control scheme. Firstly, exponential convergence rates can be achieved. Secondly, this method is not restricted to the zero total angular momentum assumption that most existing underactuated control techniques exploit.

The conference paper [26] reported our preliminary results, which are significantly extended in this paper. In particular, the developments proceed based on a more general spacecraft model. Additional analysis and discussions are presented, and new simulation results are included.

The paper is organized as follows. The underactuated spacecraft model is presented in Sec. II, with the attitude kinematics and dynamics derived in Secs. II.A and II.B. Angular momentum conservation is discussed in Sec. III. Base and fiber variables are defined explicitly in Sec. IV. Section V develops the switching algorithms for underactuated attitude stabilization. Specifically, Secs. V.A and V.B discuss local controllability in the fiber variable. Section V.C presents a switching scheme that can stabilize an underactuated spacecraft when there is no angular momentum along the uncontrollable axis, and convergence properties are discussed in Sec. V.D. Section V.E presents an alternative switching algorithm for controlled oscillations in a neighborhood around the target pointing configuration when there is a nonzero total angular momentum component along the uncontrollable axis. The motions of the underactuated spacecraft are then analyzed and their asymptotic properties are characterized under high-frequency base dynamic excitations in Sec. VI. Results from simulating the switching schemes on the full nonlinear model are presented in Sec. VII. Concluding remarks are made in Sec. VIII.

Throughout this paper the following notation is used. Frames are denoted by script, $\mathcal{S}$. If a physical vector $\boldsymbol{r}$ is resolved in frame $\mathcal{S}$ and becomes a mathematical vector r, then the notation $r = \boldsymbol{r}|_{\mathcal{S}}$ is used. Physical unit vectors are expressed with an overscript hat $\hat{r}$. The notation for a mathematical vector obtained by resolving a physical vector $\boldsymbol{r}$ in a given frame $\mathcal{S}$ is $\boldsymbol{r}|_{\mathcal{S}}$. The time derivative of a physical vector $\boldsymbol{r}$ with respect to a given frame $\mathcal{S}$ is $\overset{\mathcal{S}\cdot}{\boldsymbol{r}}$.

II. Spacecraft Modeling

In this paper, a spacecraft configuration consisting of a bus and two RWs is considered. The equations of motion are defined with the help of two reference frames:

1) An inertial frame $\mathcal{I}$ with orthogonal axes whose origin is at the center of mass (COM) of the total spacecraft assembly (including the spacecraft bus and RWs).

2) A spacecraft bus body fixed frame $\mathcal{B}$ with orthogonal axes is defined by unit axes $\hat{b}_1$, $\hat{b}_2$, and $\hat{b}_3$ and with the origin at the COM of the total spacecraft.

The physical angular velocity vector of frame $\mathcal{B}$ relative to $\mathcal{I}$ is written as

$$\boldsymbol{\omega} = \omega_1 \hat{b}_1 + \omega_2 \hat{b}_2 + \omega_3 \hat{b}_3 \tag{1}$$

and, therefore, $\omega = \boldsymbol{\omega}|_{\mathcal{B}} = [\omega_1 \quad \omega_2 \quad \omega_3]^{\mathrm{T}}$. We do not assume $\mathcal{B}$ is a principal frame. Without loss of generality, we assume that frame $\mathcal{I}$ is aligned to coincide with the desired inertial pointing attitude. The RWs spin at speeds ν_1 and ν_2 about nonparallel axes defined by $\hat{w}_1$ and $\hat{w}_2$, which are fixed in $\mathcal{B}$. We also assume that $\hat{b}_1$ and $\hat{b}_2$ lie in the plane spanned by $\hat{w}_1$ and $\hat{w}_2$. This plane may be thought of as a plane of controllability where all body-fixed torques induced by RWs must lie. The unit vector $\hat{b}_3$ is orthogonal to this plane and corresponds to the underactuated axis. Figure 1 depicts the two frames, the RW spin axes, and the plane of controllability.

A. Kinematics

The orientation of $\mathcal{B}$ relative to $\mathcal{I}$ is characterized by three successive rotations, defined by 3-2-1 Euler angles ψ (yaw), θ (pitch), and ϕ (roll). It is assumed that the maneuvers being performed involve relatively small attitude adjustments near the desired pointing orientation, and, therefore, the singularities in Euler angle attitude representation are not of concern. Let $\Theta = [\phi \quad \theta \quad \psi]^T$. The spacecraft kinematic equations, following from the derivations in [27], are

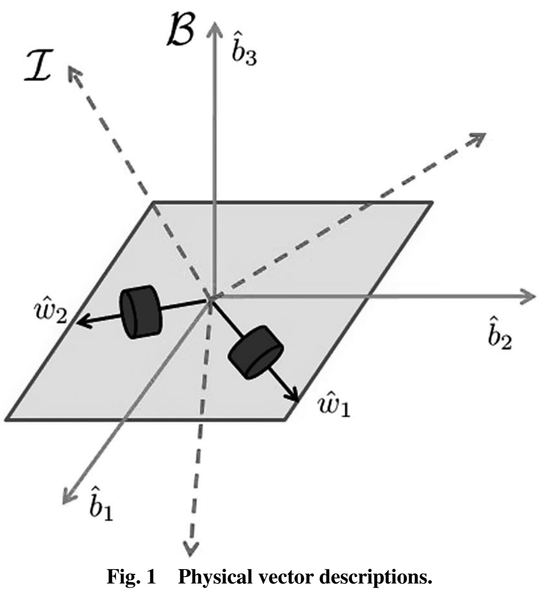

Fig. 1 Physical vector descriptions.

$$\dot{\Theta} = M(\Theta)\omega \tag{2}$$

in which

$$M(\Theta) = \frac{1}{\theta_c}\begin{bmatrix} \theta_c & \phi_s\theta_s & \phi_c\theta_s \\ 0 & \phi_c\theta_c & -\phi_s\theta_c \\ 0 & \phi_s & \phi_c \end{bmatrix} \tag{3}$$

In Eq. (3), $(*)_c = \cos(*)$ and $(*)_s = \sin(*)$.

B. Dynamics of the Spacecraft

The dynamics of the spacecraft are derived from the relation

$$\overset{\mathcal{I}\cdot}{\boldsymbol{H}} = \boldsymbol{M}_{\text{ext}} \tag{4}$$

in which $\boldsymbol{H}$ is the total spacecraft's angular momentum and $\boldsymbol{M}_{\text{ext}}$ is the total external moment about the COM of the spacecraft assembly. Let $\bar{J}_0$, $\bar{J}_{w1}$, and $\bar{J}_{w2}$ be the inertia matrices of the spacecraft bus, RW 1, and RW 2, each relative to the COM of the spacecraft assembly and expressed in $\mathcal{B}$. Furthermore, let J_{s1} and J_{s2} be the inertias of RW 1 and RW 2 about their respective spin axes corresponding to unit vectors $\hat{w}_1$ and $\hat{w}_2$. If $H = \boldsymbol{H}|_{\mathcal{I}}$, then H is related to ω, ν_1, and ν_2 by

$$\mathcal{O}_{\mathcal{B}/\mathcal{I}} H = \bar{J}\omega + \bar{W}\nu \tag{5}$$

in which

$$\begin{aligned} \bar{J} &= \bar{J}_0 + \bar{J}_{w1} + \bar{J}_{w2}, \\ \bar{W} &= W J_s, \\ W &= [\hat{w}_1|_{\mathcal{B}} \quad \hat{w}_2|_{\mathcal{B}}], \\ J_s &= \operatorname{diag}(J_{s1}, J_{s2}), \\ \nu &= [\nu_1 \quad \nu_2]^T, \\ \mathcal{O}_{\mathcal{B}/\mathcal{I}} &= \begin{bmatrix} \theta_c\psi_c & \theta_c\psi_s & -\theta_s \\ \phi_s\theta_s\psi_c - \phi_c\psi_s & \phi_s\theta_s\psi_s + \phi_c\psi_c & \phi_s\theta_c \\ \phi_c\theta_s\psi_c + \phi_s\psi_s & \phi_c\theta_s\psi_s - \phi_s\psi_c & \phi_c\theta_c \end{bmatrix} \end{aligned} \tag{6}$$

Each of the variables in Eq. (6) has a physical significance. The matrix $\bar{J}$ is the total inertia of the spacecraft assembly about its COM. The columns of $\bar{W}$ define how much influence each RW has on the spacecraft and in what direction. The matrix $\mathcal{O}_{\mathcal{B}/\mathcal{I}}$ specifies the orientation of frame $\mathcal{B}$ relative to $\mathcal{I}$.

It follows from Eqs. (4) and (5), as well as the derivations in [5], that the dynamic equations of motion are of the form

$$\bar{J}\dot{\omega} = -\omega \times (\bar{J}\omega + \bar{W}\nu) - \bar{W}\dot{\nu} + M_{\text{ext}} \tag{7}$$

in which $M_{\text{ext}} = \boldsymbol{M}_{\text{ext}}|_{\mathcal{B}}$. In this work, the RW accelerations are treated as the control inputs,

$$\dot{\nu} = u \tag{8}$$

Let the total inertia matrix $\bar{J}$ have the following form,

$$\bar{J} = \begin{bmatrix} j_{11} & j_{12} & j_{13} \\ j_{12} & j_{22} & j_{23} \\ j_{13} & j_{23} & j_{33} \end{bmatrix} \tag{9}$$

which will be useful in the derivation and analysis of the switching controller.

III. Angular Momentum Conservation Law

Consider the case of an underactuated spacecraft that does not experience any external moments (i.e., $\boldsymbol{M}_{\text{ext}} = 0$). Equation (4) then implies that the total angular momentum is conserved. Proposition 1 presents a requirement for $\Theta = \omega = 0$ to be an equilibrium, which corresponds to maintaining inertial pointing at the desired attitude.

Proposition 1: Let $H = [h_1 \quad h_2 \quad h_3]^T$ and assume that $M_{\text{ext}} = 0$ for an underactuated spacecraft satisfying the above assumptions. Then $\Theta = \omega = 0$ is an equilibrium if and only if $h_3 = 0$.

Proof: If $\Theta(t) = \omega(t) = 0$ for all t, then Eq. (5) reduces to

$$H = \bar{W}\nu \tag{10}$$

If the spacecraft fixed frame $\mathcal{B}$ is defined as in Sec. II, then $[0 \quad 0 \quad 1]\bar{W}\nu = 0$. Premultiplying Eq. (10) by $[0 \quad 0 \quad 1]$ yields

$$h_3 = 0 \tag{11}$$

□

We make the assumption throughout this paper that the total angular momentum is conserved, but we do not require that $H = 0$.

The angular velocity component ω_3 can also be found from the angular momentum expression in Eq. (5). Define $\zeta_1 = [\omega_1 \quad \omega_2 \quad 0]^T$ and $\zeta_2 = [\nu^T \quad \omega_3]^T$. Then Eq. (5) can be written as

$$\mathcal{O}_{\mathcal{B}/\mathcal{I}}H - \bar{J}Z_1\zeta_1 = (\bar{J}Z_2 + \bar{W}Z_3)\zeta_2 \tag{12}$$

in which

$$Z_1 = \begin{bmatrix} I_{2\times2} \\ 0_{1\times2} \end{bmatrix}, \quad Z_2 = \text{diag}(0,0,1), \quad Z_3 = [I_{2\times2} \quad 0_{2\times1}] \tag{13}$$

Solving for ζ_2 and extracting ω_3 gives

$$\omega_3 = -\frac{j_{13}}{j_{33}}\omega_1 - \frac{j_{23}}{j_{33}}\omega_2 + \frac{h_1}{j_{33}}(\phi_c\theta_s\psi_c + \phi_s\psi_s) + \frac{h_2}{j_{33}}(\phi_c\theta_s\psi_s - \phi_s\psi_c) + \frac{h_3}{j_{33}}\phi_c\theta_c \tag{14}$$

IV. Base and Fiber Variables

In the following switching scheme, the six-dimensional state vector, consisting of Euler angles and angular velocities, is divided into base variables and fiber variables. The base variables are chosen to be the controllable variables ϕ, θ, ω_1, and ω_2. The uncontrolled angle ψ is treated as a fiber variable. The reason why ω_3 is not included in either the base of fiber variables is mentioned in Sec. IV.B.

A. Base Variables

Consider a small angle assumption for the kinematics of ϕ and θ in Eq. (2). This results in $\dot{\phi} = \omega_1$ and $\dot{\theta} = \omega_2$. Also, let the RW accelerations be determined by the feedback law

$$u = (Z_3\bar{J}^{-1}\bar{W})^{-1}(Z_3\bar{J}^{-1}(-\omega \times (\bar{J}\omega + \bar{W}\nu)) + (v_{\text{fb}} - v)) \tag{15}$$

in which

$$v_{\text{fb}} = \begin{bmatrix} k_{11}\phi + k_{12}\omega_1 \\ k_{21}\theta + k_{22}\omega_2 \end{bmatrix}, \qquad v = \begin{bmatrix} v_1 \\ v_2 \end{bmatrix} \tag{16}$$

Z_3 is from Eq. (13), and k_{11}, k_{12}, k_{21}, and k_{22} are constants. Under the above control law and by defining $x = [\phi \quad \omega_1 \quad \theta \quad \omega_2]^T$, the base dynamics can be written as a linear system,

$$\dot{x} = Ax + Bv \tag{17}$$

in which

$$A = \begin{bmatrix} 0 & 1 & 0 & 0 \\ -k_{11} & -k_{12} & 0 & 0 \\ 0 & 0 & 0 & 1 \\ 0 & 0 & -k_{21} & -k_{22} \end{bmatrix}, \qquad B = \begin{bmatrix} 0 & 0 \\ 1 & 0 \\ 0 & 0 \\ 0 & 1 \end{bmatrix} \tag{18}$$

The constants k_{11}, k_{12}, k_{21}, and k_{22} are chosen to make A Hurwitz.

Now let the base variables be excited by the $T = \frac{2\pi}{n}$ periodic inputs,

$$v_1 = \alpha_1(nt + \delta_1)_c, \quad v_2 = \alpha_2(nt + \delta_2)_c \tag{19}$$

in which n is the excitation frequency and α_1, α_2, δ_1, and δ_2 are parameters. Because the base dynamics are exponentially stable, the steady-state trajectories of Eq. (17) induced by the inputs in Eq. (19) will be periodic and at the excitation frequency determined by

$$x_{\text{ss}}(t) = Re\left\{(njI_{4\times4} - A)^{-1}B\begin{bmatrix} \alpha_1 \exp(j\delta_1) \\ \alpha_2 \exp(j\delta_2) \end{bmatrix}\exp(jnt)\right\} \tag{20}$$

in which $Re\{*\}$ denotes the real part. More specifically, these steady-state trajectories have the following form:

$$\bar{x}(t) = \begin{bmatrix} \bar{\phi}(t) \\ \bar{\omega}_1(t) \\ \bar{\theta}(t) \\ \bar{\omega}_2(t) \end{bmatrix} = \begin{bmatrix} \alpha_1\beta_1(nt + \delta_1 + \gamma_1)_c \\ \alpha_1\beta_2(nt + \delta_1 + \gamma_2)_c \\ \alpha_2\beta_3(nt + \delta_2 + \gamma_3)_c \\ \alpha_2\beta_4(nt + \delta_2 + \gamma_4)_c \end{bmatrix} \tag{21}$$

in which

$$\begin{aligned} \beta_1 &= |k_{11}^2 - 2k_{11}n^2 + k_{12}^2n^2 + n^4|^{-\frac{1}{2}}, \\ \beta_2 &= n|k_{11}^2 - 2k_{11}n^2 + k_{12}^2n^2 + n^4|^{-\frac{1}{2}}, \\ \beta_3 &= |k_{21}^2 - 2k_{21}n^2 + k_{22}^2n^2 + n^4|^{-\frac{1}{2}}, \\ \beta_4 &= n|k_{21}^2 - 2k_{21}n^2 + k_{22}^2n^2 + n^4|^{-\frac{1}{2}} \end{aligned} \tag{22}$$

$$\begin{aligned} \gamma_1 &= \tan^{-1}\left(\frac{-nk_{12}}{k_{11} - n^2}\right), \\ \gamma_2 &= \tan^{-1}\left(\frac{-n^2 + k_{11}}{nk_{12}}\right), \\ \gamma_3 &= \tan^{-1}\left(\frac{-nk_{22}}{k_{21} - n^2}\right), \\ \gamma_4 &= \tan^{-1}\left(\frac{-n^2 + k_{21}}{nk_{22}}\right) \end{aligned} \tag{23}$$

In the sequel, δ_1 and δ_2 are constants chosen by the designer, whereas α_1 and α_2 are treated as new control parameters that are adjusted at every periodic cycle.

B. Fiber Variables

We treat ψ as the only fiber variable in our switching scheme. Note that ω_3 is determined by Eq. (14), and hence we choose not to consider it as a fiber variable explicitly. To control ψ, its change over one period of excitation induced by steady-state base variable motions needs to be characterized. If the base variables are in steady-state, ψ evolves in time according to

$$\dot{\psi} = \bar{\omega}_2\bar{\phi}_s\bar{\theta}_{se} + \left(-\frac{j_{13}}{j_{33}}\bar{\omega}_1 - \frac{j_{23}}{j_{33}}\bar{\omega}_2\right)\bar{\phi}_c\bar{\theta}_{se} + \left(\frac{h_1}{j_{33}}(\bar{\phi}_c\bar{\theta}_s\psi_c + \bar{\phi}_s\psi_s) + \frac{h_2}{j_{33}}(\bar{\phi}_c\bar{\theta}_s\psi_s - \bar{\phi}_s\psi_c) + \frac{h_3}{j_{33}}\bar{\phi}_c\bar{\theta}_c\right)\bar{\phi}_c\bar{\theta}_{se} \tag{24}$$

in which $\bar{\phi}$, $\bar{\theta}$, $\bar{\omega}_1$, and $\bar{\omega}_2$ are the steady-state trajectories from Eq. (21) and $\sec(*) = *_{se}$. Assuming small angles allows simplification of Eq. (24) to

$$\dot{\psi}=\left(\frac{h_1}{j_{33}}\bar{\phi}+\frac{h_2}{j_{33}}\bar{\theta}\right)\psi+\bar{\omega}_2\bar{\phi}+\frac{h_1}{j_{33}}\bar{\theta}-\frac{h_2}{j_{33}}\bar{\phi}-\frac{j_{13}}{j_{33}}\bar{\omega}_1-\frac{j_{23}}{j_{33}}\bar{\omega}_2+\frac{h_3}{j_{33}} \tag{25}$$

Using Eq. (21), Eq. (25) becomes

$$\begin{aligned}\dot{\psi}=&\left(\frac{h_1\alpha\beta_1}{j_{33}}(nt+\delta_1+\gamma_1)_c+\frac{h_2\alpha_2\beta_3}{j_{33}}(nt+\delta_2+\gamma_3)_c\right)\psi\\&+\alpha_1\alpha_2\beta_1\beta_4(nt+\delta_1+\gamma_1)_c(nt+\delta_2+\gamma_4)_c\\&+\frac{h_1\alpha_2\beta_3}{j_{33}}(nt+\delta_2+\gamma_3)_c-\frac{h_2\alpha_1\beta_1}{j_{33}}(nt+\delta_1+\gamma_1)_c\\&-\frac{\alpha_1\beta_2 j_{13}}{j_{33}}(nt+\delta_1+\gamma_2)_c-\frac{j_{23}\alpha_2\beta_4}{j_{33}}(nt+\delta_2+\gamma_4)_c+\frac{h_3}{j_{33}}\end{aligned} \tag{26}$$

We note that while the approximations in Eqs. (25) and (26) are used as a basis for the subsequent control law design, the simulation results in Sec. VII are performed on the original nonlinear model, given by Eqs. (2), (7), and (8).

V. Switching Feedback Law

We now develop a switching feedback law that adjusts parameters of periodic excitation amplitude of the base dynamics (α_1 and α_2), in order to induce a change in the fiber variable (ψ) toward the desired pointing equilibrium. The switching feedback law construction is based on [24] and relies on the characterization of the change in ψ induced by one cycle of periodic, steady-state base variable motion.

Let the exact change in ψ, determined by the integration of Eq. (24), be denoted as $\Delta\psi$. Note that Eq. (24) cannot be analytically integrated. Thus an approximation of $\Delta\psi$, denoted as $\Delta_a\psi$ and based on the integration of Eq. (26), is used for analysis.

Two cases are considered when analyzing $\Delta_a\psi$. First studied is the zero total angular momentum case (i.e. $h_1 = h_2 = h_3 = 0$), which yields an exact integration of Eq. (26). Then the nonzero total angular momentum with $h_3 = 0$ (consistent with proposition 1) is studied using a second-order Taylor series expansion. In both cases, it is required that the mapping G_a: $(\alpha_1, \alpha_2) \to \Delta_a\psi$ be open at $(\alpha_1, \alpha_2) = (0, 0)$ [i.e., an image of an open neighborhood of $(\alpha_1, \alpha_2) = (0, 0)$] is an open interval, and hence the change of ψ over one period of steady-state base variable motion can be made in any direction, regardless of how small the magnitude of α_1 and α_2 is. This can be seen as a controllability-like property of the fiber variables by periodic base variable motions. It is shown that if G_a is open at $(\alpha_1, \alpha_2) = (0, 0)$, then the map for the actual change in ψ, defined as G: $(\alpha_1, \alpha_2) \to \Delta\psi$, is also open at $(\alpha_1, \alpha_2) = (0, 0)$.

A. Zero Inertial Angular Momentum

If $h_1 = h_2 = h_3 = 0$, Eq. (26) reduces to

$$\begin{aligned}\dot{\psi}=&\,\alpha_1\alpha_2\beta_1\beta_4(nt+\delta_1+\gamma_1)_c(nt+\delta_2+\gamma_4)_c\\&-\frac{\alpha_1\beta_2 j_{13}}{j_{33}}(nt+\delta_1+\gamma_2)_c-\frac{j_{23}\alpha_2\beta_4}{j_{33}}(nt+\delta_2+\gamma_4)_c\end{aligned} \tag{27}$$

The right side of Eq. (27) is not a function of ψ. The change in ψ induced by one period of steady-state base variable motion is then approximated as

$$\Delta_a\psi = \alpha_1\alpha_2\Gamma \tag{28}$$

in which

$$\Gamma = \frac{\pi\beta_1\beta_4}{n}(\delta_1 - \delta_2 + \gamma_1 - \gamma_4)_c \tag{29}$$

Note that Eq. (27) defines a function of α_1 and α_2, with all other parameters considered fixed. Assuming that $\Gamma \neq 0$, which can be assured by choosing suitable values for $k_{11}, k_{12}, k_{21}, k_{22}, \delta_1$, and δ_2, it follows that the map G_a is open at $(\alpha_1, \alpha_2) = (0, 0)$.

We note that the derivation of Eq. (28) relies on the assumption of small angles that was made in obtaining Eqs. (25) and (26). The predicted change $\Delta_a\psi$ is very close to $\Delta\psi$, provided that α_1 and α_2 are sufficiently small. Figure 2 demonstrates this by showing the change predicted by Eq. (28) (represented by the dashed line in Fig. 2a) along with a numerical integration of Eq. (24) (represented by the solid line in Fig. 2a) using the spacecraft parameters outlined in Sec. VII.A and the controller parameters listed in the table in Sec. VII.

B. Nonzero Inertial Angular Momentum with $h_3 = 0$

Suppose now h_1 and/or h_2 is nonzero while $h_3 = 0$, which is the case consistent with proposition 1. Note that Eq. (26) is linear with respect to ψ. Because Eq. (26) is also a scalar differential equation, its state transition matrix is computed as

$$\begin{aligned}\Phi(t,t_0)=&\exp\left(\frac{h_1\alpha_1\beta_1}{nj_{33}}(nt+\delta_1+\gamma_1)_s+\frac{h_2\alpha_2\beta_3}{nj_{33}}(nt+\delta_2+\gamma_3)_s\right)\\&*\exp\left(-\frac{h_1\alpha_1\beta_1}{nj_{33}}(nt_0+\delta_1+\gamma_1)_s-\frac{h_2\alpha_2\beta_3}{nj_{33}}(nt_0+\delta_2+\gamma_3)_s\right)\end{aligned} \tag{30}$$

Note that the state transition matrix is T periodic. Thus the change in ψ over one period does not depend on the initial state at the beginning of the period. Then

$$\Delta_a\psi = \int_0^T \Phi(t,\tau)b(\tau)\,\mathrm{d}\tau \tag{31}$$

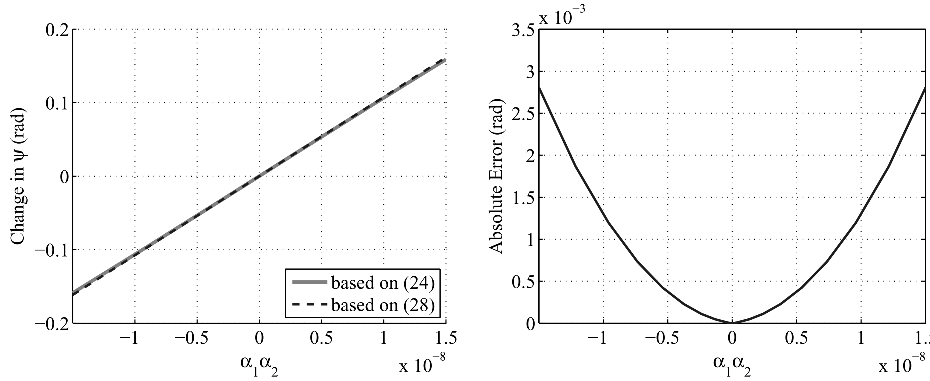

a) Exact vs. approximate change b) Error Magnitude

Fig. 2 Change in ψ due to periodic base dynamic excitation for $H = 0$.

in which

$$
\begin{aligned}
b(\tau) = {} & \alpha_1\alpha_2\beta_1\beta_4(n\tau+\delta_1+\gamma_1)_c(n\tau+\delta_2+\gamma_4)_c \\
& + \frac{h_1\alpha_2\beta_3}{j_{33}}(n\tau+\delta_2+\gamma_3)_c - \frac{h_2\alpha_1\beta_1}{j_{33}}(n\tau+\delta_1+\gamma_1)_c \\
& - \frac{\alpha_1\beta_2 j_{13}}{j_{33}}(nt+\delta_1+\gamma_2)_c - \frac{j_{23}\alpha_2\beta_4}{j_{33}}(nt+\delta_2+\gamma_4)_c
\end{aligned}
\tag{32}
$$

Although $\Delta_a\psi$ can be constructed by fitting numerical values, it turns out that accurate analytical approximations can also be developed. For sufficiently small α_1 and α_2, a second-order Taylor series expansion about $\alpha_1 = \alpha_2 = 0$ can approximate Eq. (31),

$$\Delta_a\psi = \alpha^T \Xi \alpha \tag{33}$$

in which

$$
\begin{aligned}
\alpha &= [\alpha_1 \ \ \alpha_2]^T, \\
\Xi &= \begin{bmatrix} \Gamma_1 & \frac{1}{2}\Gamma_3 \\ \frac{1}{2}\Gamma_3 & \Gamma_2 \end{bmatrix}, \\
\Gamma_1 &= \frac{\pi j_{13}\beta_1\beta_2 h_1}{j_{33}^2 n^2}(\gamma_1-\gamma_2)_s, \\
\Gamma_2 &= \frac{\pi j_{23}\beta_3\beta_4 h_2}{j_{33}^2 n^2}(\gamma_3-\gamma_4)_s, \\
\Gamma_3 &= \frac{\pi\beta_1\beta_4}{n}(\delta_1-\delta_2+\gamma_1-\gamma_4)_c - \frac{\pi\beta_1\beta_3}{j_{33}^2 n^2}(h_1^2+h_2^2)(\delta_1-\delta_2+\gamma_1-\gamma_3)_s \\
&\quad - \frac{\pi j_{13}\beta_2\beta_3 h_2}{j_{33}^2 n^2}(\delta_1-\delta_2+\gamma_2-\gamma_3)_s + \frac{\pi j_{23}\beta_1\beta_4 h_1}{j_{33}^2 n^2}(\delta_1-\delta_2+\gamma_1-\gamma_4)_s
\end{aligned}
\tag{34}
$$

Note that the map G_a given by Eq. (33) is open at $(\alpha_1, \alpha_2) = (0, 0)$ if the symmetric matrix Ξ is indefinite (i.e., has a positive and a negative eigenvalue). Under this condition, which can be satisfied by choosing suitable values for k_{11}, k_{12}, k_{21}, k_{22}, δ_1, and δ_2, the exact map G can also be shown to be open at $(\alpha_1, \alpha_2) = (0, 0)$. Note that (28) is recovered from (33) if $h_1 = h_2 = 0$.

Figure 3 shows, based on the spacecraft parameters in Sec. VII.A and control parameters in the table, that when $h_1 = h_2 = 1\ \mathrm{kg\cdot m^2/s}$ and $h_3 = 0$ the approximation $\Delta_a\psi$ from (33) (represented by the dashed line in Fig. 3a) is fairly accurate to the actual change $\Delta\psi$ (represented by the solid line in Fig. 3a) and that the mapping is open at $(\alpha_1, \alpha_2) = (0, 0)$.

C. Hybrid Controller Scheme

A switching scheme, based on [24], that stabilizes the fiber and base variables is now implemented for the case when $h_3 = 0$. This is consistent with proposition 1, and hence stabilization to the desired pointing equilibrium is possible. The parameters that this algorithm concerns itself with are α_2 and ϵ, with $\alpha_1 = \epsilon\alpha_2$. Each of these parameters are adjusted at the beginning of time duration T and are kept constant throughout the cycle,

$$
\begin{aligned}
\alpha_2(t) &= \alpha_2(kT) = \alpha_2^k, \qquad kT \le t < (k+1)T, \\
\epsilon(t) &= \epsilon(kT) = \epsilon^k, \qquad kT \le t < (k+1)T
\end{aligned}
\tag{35}
$$

Let $k \ge 0$ represent the cycle number, $\psi^k = \psi(kT)$, and choose $\mu_1 \in (0, 1)$, ξ_1 to be sufficiently small, and ξ_2 to be such that $\xi_1\xi_2$ is sufficiently small. The switching scheme is then outlined by Algorithm 1. Note that the computation involved for α_1, α_2, v_1, v_2, and the control law in Eq. (15) rely on closed-form, algebraic manipulations that do not require much processing power to execute.

Algorithm 1 Control computation for $h_3 = 0$

Given:
  $k \ge 0$, $\mu_1 \in (0, 1)$, ξ_1 sufficiently small, and ξ_2 such that $\xi_1\xi_2$ is sufficiently small
if $k = 0$ **then**
  if $\psi^k = 0$ **then**
    $\alpha_2^k = 0$, $\epsilon^k = 0$
  else
    $\alpha_2^k = \xi_1$, $\epsilon^k = -\xi_2 \mathrm{sign}(\Gamma_3\psi^0)$
  end if
else $\{k > 0\}$
  Compute $G_a(\epsilon^{k-1}\alpha_2^{k-1}, \alpha_2^{k-1})\psi^k$ using Eq. (33)
  if $\psi^k = 0$ **or** $G_a(\epsilon^{k-1}\alpha_2^{k-1}, \alpha_2^{k-1})\psi^k < 0$ **then**
    $\alpha^k = \alpha_2^{k-1}$, $\epsilon^k = \epsilon^{k-1}$
  else $\{G_a(\epsilon^{k-1}\alpha_2^{k-1}, \alpha_2^{k-1})\psi^k \ge 0\}$
    $\alpha^k = \mu_1\alpha_2^{k-1}$, $\epsilon^k = -\epsilon^{k-1}$,
  end if
end if
Control During Cycle k:
  $v_1(t) = \alpha_2^k\epsilon^k(nt+\delta_1)_c$, $v_2(t) = \alpha_2^k(nt+\delta_2)_c$, $v(t) = [v_1(t) \quad v_2(t)]^T$ for $t \in [kT, (k+1)T)$
  Compute $u(t)$ from the feedback law in Eq. (15)

The methodology of Algorithm 1 is as follows. The sign of ϵ dictates the direction of $\Delta_a\psi$ (which can be seen from Figs. 2 and 3). Furthermore, the magnitude of $\Delta_a\psi$ is dictated by α_2. If the direction of $\Delta_a\psi$ is to be reversed, the sign of ϵ is changed and the magnitude of α_2 is reduced by a factor of μ_1. As α_2 approaches zero so does ψ, which in turn causes the base variables to converge to zero. The initial values for α_2 and ϵ (i.e., α_2^0 and ϵ^0) are governed by ξ_1 and ξ_2, which are chosen so as to not cause large transients in ψ.

D. Convergence Properties

In [24], global asymptotic convergence was proven for a cascade connection of a linear time-invariant subsystem, representing the

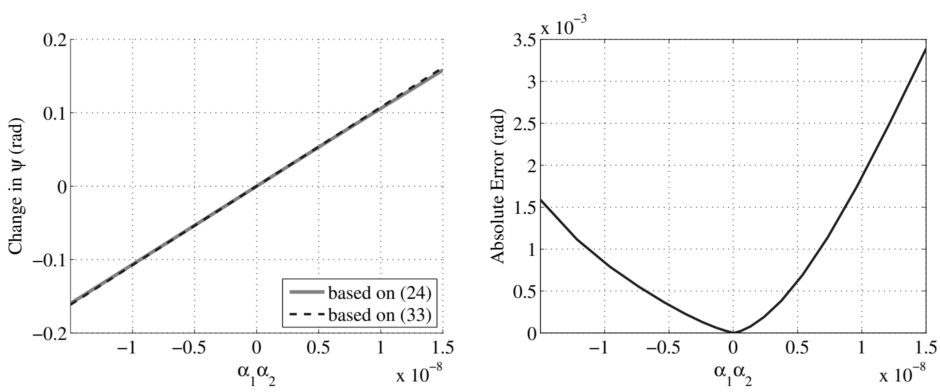

a) Exact vs. approximate change b) Error Magnitude

Fig. 3 Change in ψ due to periodic base dynamic excitation for $H = [1 \quad 1 \quad 0]^T\ \mathrm{kg\cdot m^2/s}$.

base dynamics, and a subsystem of nonlinear integrators, representing the fiber dynamics. Related local stabilization results have been obtained in [25] for the more general case of fiber dynamics with drift. For the zero angular momentum case, $h_1 = h_2 = h_3 = 0$, the results in [24] can be applied directly to demonstrate exponential convergence. In the case when h_1 and/or h_2 are nonzero while $h_3 = 0$, the rationale for our switching feedback law is very similar; however, existing theoretical guarantees appear to be insufficient, in particular, due to the form of the fiber dynamics in Eq. (26) not being explicitly treated in prior publications. For the proofs in [24] to carry over to our present case, it is necessary to guarantee 1) that G_a does not rely on the initial conditions of the fiber variable and 2) the boundedness of the error between the fiber variable trajectory ψ induced by exponentially convergent base variable motions to a periodic steady-steady state and the fiber variable trajectory $\bar{\psi}$ induced by the base variable motion in the periodic steady state. Equation (30) shows that the state transition matrix is T-periodic, and therefore G_a is independent of the initial condition of ψ. Lemma 1 proves the boundedness of the error between ψ and $\bar{\psi}$ if the dynamics of the fiber variable are given by Eq. (25).

Lemma 1: Let the fiber variable dynamics for ψ be given by Eq. (25) with $h_3 = 0$. Then the error between ψ and $\bar{\psi}$ remains bounded over time.

Proof: Define $e_\psi = \psi - \bar{\psi}$. Then

$$\dot{e}_\psi = \dot{\psi} - \dot{\bar{\psi}} \tag{36}$$

Using (25) with $h_3 = 0$, Eq. (36) can be rewritten as

$$\dot{e}_\psi = \left(\frac{h_1}{j_{33}}\phi + \frac{h_2}{j_{33}}\theta\right)\psi + d(\phi, \theta, \omega_1, \omega_2) - \left(\frac{h_1}{j_{33}}\bar{\phi} + \frac{h_2}{j_{33}}\bar{\theta}\right)\bar{\psi} - d(\bar{\phi}, \bar{\theta}, \bar{\omega}_1, \bar{\omega}_2) \tag{37}$$

in which

$$d(\phi, \theta, \omega_1, \omega_2) = \omega_2\phi + \frac{h_1}{j_{33}}\theta - \frac{h_2}{j_{33}}\phi - \frac{j_{13}}{j_{33}}\omega_1 - \frac{j_{23}}{j_{33}}\omega_2 \tag{38}$$

Adding and subtracting $(\frac{h_1}{j_{33}}\bar{\phi} + \frac{h_2}{j_{33}}\bar{\theta})\psi$ from Eq. (37) and simplifying then yields

$$\dot{e}_\psi = \left(\frac{h_1}{j_{33}}\bar{\phi} + \frac{h_2}{j_{33}}\bar{\theta}\right)e_\psi + \left(\frac{h_1}{j_{33}}e_\phi + \frac{h_2}{j_{33}}e_\theta\right)\psi + (d(\phi, \theta, \omega_1, \omega_2) - d(\bar{\phi}, \bar{\theta}, \bar{\omega}_1, \bar{\omega}_2)) \tag{39}$$

in which $e_\phi = \phi - \bar{\phi}$ and $e_\theta = \theta - \bar{\theta}$. Equation (39) is linear with respect to e_ψ, and its solution at time t can be written as

$$e_\psi(t) = \Phi(t, 0)e_\psi(0) + \int_0^t \Phi(t, \tau)f(\tau)\,\mathrm{d}\tau \tag{40}$$

in which $e_\psi(0)$ is the initial error, $\Phi(t, 0)$ is the state transition matrix from Eq. (30), and

$$f(t) = \left(\frac{h_1}{j_{33}}e_\phi + \frac{h_2}{j_{33}}e_\theta\right)\psi + (d(\phi, \theta, \omega_1, \omega_2) - d(\bar{\phi}, \bar{\theta}, \bar{\omega}_1, \bar{\omega}_2)) \tag{41}$$

The base variables converge exponentially to the steady-state periodic motions, and $\psi(0)$ is initially known and bounded. The function $f(t)$ given by Eq. (41) hence converges to zero exponentially. This implies that there exists a constant $c_1 > 0$ such that

$$|e_\psi(t)| \le |\Phi(t,0)e_\psi(0)| + \int_0^t |\Phi(\tau,0)||f(\tau)|\,\mathrm{d}\tau \le |\Phi(t,0)e_\psi(0)| + c_1 \tag{42}$$

The state transition matrix $\Phi(t, 0)$ in Eq. (30) is bounded, and therefore the error e_ψ is bounded. □

We summarize the theoretical convergence guarantees as follows:

Theorem 1: Consider the fiber dynamics [in Eq. (25)] with $h_3 = 0$ and base dynamics [in Eq. (17)] with the switching controller given in Algorithm 1 and Eq. (19). Under the above assumptions, $\alpha_1^k, \alpha_2^k \to 0$ as $k \to \infty$, and $\phi(t), \theta(t), \psi(t) \to 0$ as $t \to \infty$. □

Remark 1: The development and analysis of convergence for the above controller have relied on small angle approximation to simplify the representation for the base variable kinematics and fiber variable dynamics. Our subsequent simulations are performed on a model that does not use these approximations, thereby validating these desirable convergence properties. Note also the theoretical results in [24] allow for inexact knowledge of G in maintaining convergence properties.

E. Switching Scheme When $h_3 \neq 0$

Now consider the case when $h_3 \neq 0$. Stabilization at $\Theta = \omega = 0$ is not possible by proposition 1 (i.e., it violates the law of angular momentum conservation). If $\alpha_1 = \alpha_2 = 0$ at $\Theta = \omega = 0$, Eq. (24) becomes

$$\dot{\psi} = \frac{h_3}{j_{33}} \tag{43}$$

which can be integrated over one steady-state cycle to give

$$\Delta\psi = \frac{2\pi h_3}{n j_{33}} \tag{44}$$

Equation (44) shows that G is not open at $(\alpha_1, \alpha_2) = (0, 0)$, and thus Algorithm 1 cannot be used. By modifying the algorithm, however, controlled oscillations of Euler angles in the neighborhood of $\Theta = 0$ can be achieved.

Remark 2: The fact that G is not open in the case of $h_3 \neq 0$ gives insight into the system's controllability. In this case, if α_1 and α_2 are made arbitrarily small, then the drift in ψ can only be induced in one direction. This is in contrast to the case of $h_3 = 0$, in which a controlled drift in ψ can be made in both directions regardless of how small α_1 and α_2 are.

Let the approximation of the change in ψ induced by one steady-state cycle of base variable motions when $h_3 \neq 0$ be denoted by $\Delta_{a,h_3}\psi$ and define the map G_{a,h_3}: $(\alpha_1, \alpha_2) \to \Delta_{a,h_3}\psi$. This approximation is based on Eq. (26) and the small angles assumption. Note that, even if $h_3 \neq 0$, the state transition matrix for Eq. (26) remains the same as in Eq. (30). Then

$$\Delta_{a,h_3}\psi = \int_0^T \Phi(T, \tau)\left(b(\tau) + \frac{h_{33}}{j_{33}}\right)\mathrm{d}\tau \tag{45}$$

in which $b(t)$ is defined in Eq. (32). Performing a second-order Taylor series expansion of Eq. (45) about $(\alpha_1, \alpha_2) = (0, 0)$, $\Delta\psi$ for sufficiently small α_1 and α_2 can be approximated by

$$\Delta_{a,h_3}\psi = \bar{\Gamma}_0 + \bar{\Gamma}_{1,1}\alpha_1 + \bar{\Gamma}_{1,2}\alpha_2 + (\Gamma_1 + \bar{\Gamma}_{2,1})\alpha_1^2 + (\Gamma_2 + \bar{\Gamma}_{2,2})\alpha_2^2 + (\Gamma_3 + \bar{\Gamma}_{2,3})\alpha_1\alpha_2 \tag{46}$$

in which Γ_1, Γ_2, and Γ_3 are given in Eq. (34) and

$$
\begin{aligned}
\bar{\Gamma}_0 &= \frac{2\pi h_3}{j_{33} n},\\
\bar{\Gamma}_{1,1} &= \frac{2\pi\beta_1 h_1 h_3}{j_{33}^2 n^2}(\delta_1+\gamma_1)_s,\\
\bar{\Gamma}_{1,2} &= \frac{2\pi\beta_3 h_2 h_3}{j_{33}^2 n^2}(\delta_2+\gamma_3)_s,\\
\bar{\Gamma}_{2,1} &= \frac{\pi\beta_1^2 h_1^2 h_3}{2 j_{33}^3 n^3}(1+2(\delta_1+\gamma_1)_s^2),\\
\bar{\Gamma}_{2,2} &= \frac{\pi\beta_3^2 h_2^2 h_3}{2 j_{33}^3 n^3}(1+2(\delta_2+\gamma_3)_s^2),\\
\bar{\Gamma}_{2,3} &= -\frac{\pi\beta_1\beta_3 h_1 h_2 h_3}{j_{33}^3 n^3}((\delta_1+\delta_2+\gamma_1+\gamma_3)_c\\
&\quad - 2(\delta_1-\delta_2+\gamma_1-\gamma_3)_c)
\end{aligned}
\tag{47}
$$

Let $\alpha_1 = \epsilon\alpha_2$. Then Eq. (46) implies

$$\Delta_{a,h_3}\psi = \Lambda_c + \Lambda_b\alpha_2 + \Lambda_a\alpha_2^2 \tag{48}$$

in which

$$
\begin{aligned}
\Lambda_a &= (\Gamma_1+\bar{\Gamma}_{2,1})\epsilon^2 + (\Gamma_2+\bar{\Gamma}_{2,2}) + (\Gamma_3+\bar{\Gamma}_{2,3})\epsilon,\\
\Lambda_b &= \bar{\Gamma}_{1,1}\epsilon + \bar{\Gamma}_{1,2},\\
\Lambda_c &= \bar{\Gamma}_0
\end{aligned}
\tag{49}
$$

Because Eq. (48) is quadratic in α_2, the equation $\Delta_{a,h_3}\psi = 0$ can be solved if a specific constant ϵ_e is chosen. Denote $\alpha_{2,e}$ as a solution to $\Delta_{a,h_3}\psi = 0$ in Eq. (48) when $\epsilon = \epsilon_e$ in Eq. (49). By selecting k_{11}, k_{12}, k_{21}, k_{22}, δ_1, δ_2, and ϵ_e appropriately, Eq. (48) will have a positive real solution. The significance of $\alpha_{2,e}$ is that it corresponds to the periodic excitation of the base dynamics, which on average counteracts the drift caused by $h_3 \neq 0$. Let $\alpha_2 = \alpha_{2,e} + \delta\alpha_{2,e}$. Because $G_{a,h_3}(\epsilon_e\alpha_{2,e}, \alpha_{2,e}) = 0$, Eq. (48) can be rewritten as

$$\Delta_{a,h_3}\psi = \bar{\Lambda}_1\delta\alpha_{2,e} + \bar{\Lambda}_2\delta\alpha_{2,e}^2 \tag{50}$$

in which

$$
\begin{aligned}
\bar{\Lambda}_1 &= \bar{\Gamma}_{1,1}\epsilon_e + \bar{\Gamma}_{1,2} + 2\alpha_{2,e}((\Gamma_1+\bar{\Gamma}_{2,1})\epsilon_e^2 + (\Gamma_2+\bar{\Gamma}_{2,2}) + (\Gamma_3+\bar{\Gamma}_{2,3})\epsilon_e),\\
\bar{\Lambda}_2 &= (\Gamma_1+\bar{\Gamma}_{2,1})\epsilon_e^2 + (\Gamma_2+\bar{\Gamma}_{2,2}) + (\Gamma_3+\bar{\Gamma}_{2,3})\epsilon_e
\end{aligned}
\tag{51}
$$

Define the map $G_{a,\delta\alpha_{2,e}}$: $\delta\alpha_{2,e} \to \Delta_{a,h_3}\psi$. If $\delta\alpha_{2,e}$ is sufficiently small, the linear term in (50) dominates the quadratic term. Therefore $G_{a,\delta\alpha_{2,e}}$ is open at $\delta\alpha_{2,e} = 0$ provided that $\bar{\Lambda}_1 \neq 0$.

Now the modified switching scheme is described. Let $\delta\alpha_{2,e}$ be adjusted at the beginning of each time interval of length T and held constant:

$$\delta\alpha_{2,e}(t) = \delta\alpha_{2,e}(kT) = \delta\alpha_{2,e}^k, \qquad kT \le t < (k+1)T \tag{52}$$

Furthermore, let $\mu_1 \in (0,1)$, μ_2 be sufficiently small, and $\xi_3 > \mu_2$ be such that $|\bar{\Lambda}_1\xi_3| > |\bar{\Lambda}_2\xi_3^2|$. Then the control scheme for the case when $h_3 \neq 0$ is outlined by Algorithm 2.

The methodology of Algorithm 2 is as follows. It can be seen that $|\Delta_{a,h_3}\psi|$ is dictated by $|\delta\alpha_{2,e}|$ whereas the direction of $\Delta_{a,h_3}\psi$ is determined by the sign of $\delta\alpha_{2,e}$. The initial value of $|\delta\alpha_{2,e}^0|$ is determined by ξ_3, and it can be shown that $|\delta\alpha_{2,e}^k|$ is nonincreasing. Furthermore, as $k \to \infty$, $|\delta\alpha_{2,e}^k| \to \mu_2$, and, in the limit, α_2^k can assume either the value of $\alpha_{2,e} + \mu_2$ or $\alpha_{2,e} - \mu_2$. This steady-state "dither" in $\delta\alpha_{2,e}^k$ is introduced to compensate for the error/uncertainty in the approximation of $\Delta\psi$ by $\Delta_{a,h_3}\psi$. The value of μ_2 must be chosen as small as possible to minimize the dither, while satisfying the following property,

$$G(\epsilon_e(\alpha_{2,e}+\mu_2), \alpha_e+\mu_2)G(\epsilon_e(\alpha_{2,e}-\mu_2), \alpha_{2,e}-\mu_2) < 0 \tag{53}$$

Algorithm 2 Control computation when $h_3 \neq 0$

Given:
$k \ge 0$, $\alpha_{2,e}$ and ϵ_e from Eqs. (48) and (49), $\mu_1 \in (0,1)$, μ_2, sufficiently small, and $\xi_3 > \mu_2$ such that $|\bar{\Lambda}_1\xi_3| > |\bar{\Lambda}_2\xi_3^2|$
if $k = 0$ **then**
  if $\psi^k = 0$ **then**
    $\delta\alpha_{2,e}^0 = 0$
  else $\{\psi^k \neq 0\}$
    $\delta\alpha_{2,e}^0 = -\xi_3\,\mathrm{sign}(\bar{\Lambda}_1\psi^0)$,
  end if
else $\{k > 0\}$
  Compute $G_{a,\delta\alpha_{2,e}}(\delta\alpha_{2,e}^{k-1})\psi^k$ using Eq. (50)
  if $\psi^k = 0$ **or** $G_{a,\delta\alpha_{2,e}}(\delta\alpha_{2,e}^{k-1})\psi^k < 0$ **then**
    $\delta\alpha_{2,e}^k = \delta\alpha_{2,e}^{k-1}$
  else $\{G_{a,\delta\alpha_{2,e}}(\delta\alpha_{2,e}^{k-1})\psi^k \ge 0\}$
    $\delta\alpha_{2,e}^k = -\min\{\mu_1\delta\alpha_{2,e}^{k-1}, \mu_2\}$
  end if
end if
Control at Cycle k:
  $\alpha_1^k = \epsilon_e(\alpha_{2,e} + \delta\alpha_{2,e}^k)$, $\alpha_2^k = \alpha_{2,e} + \delta\alpha_{2,e}^k$
  $v_1(t) = \alpha_1^k(nt+\delta_1)_c$, $v_2(t) = \alpha_2^k(nt+\delta_2)_c$, $v(t) = [\,v_1(t) \quad v_2(t)\,]^T$ for $t \in [kT, (k+1)T)$
  Compute $u(t)$ from the feedback law in Eq. (15)

for Algorithm 2 to be able to induce the changes in $\Delta\psi$ by the intended sign, even in the presence of the approximation error.

Lemma 2 is a similar result to lemma 1.

Lemma 2: Let the fiber variable dynamics for ψ be given in Eq. (25). The error between the fiber variable trajectory ψ induced by base variable motions exponentially convergent to periodic steady state and the fiber variable trajectory induced by base variable motion in periodic steady-state $\bar{\psi}$ remains bounded.

Proof: If $h_3 \neq 0$, then Eq. (38) in the proof of lemma 1 changes to

$$d_{h_3}(\phi,\theta,\omega_1,\omega_2) = \omega_2\phi + \frac{h_1}{j_{33}}\theta - \frac{h_2}{j_{33}}\phi - \frac{j_{13}}{j_{33}}\omega_1 - \frac{j_{23}}{j_{33}}\omega_2 + \frac{h_3}{j_{33}} \tag{54}$$

and Eq. (41) changes to

$$
\begin{aligned}
f_{h_3}(t) &= \left(\frac{h_1}{j_{33}}e_\phi + \frac{h_2}{j_{33}}e_\theta\right)\psi + (d_{h_3}(\phi,\theta,\omega_1,\omega_2)\\
&\quad - d_{h_3}(\bar{\phi},\bar{\theta},\bar{\omega}_1,\bar{\omega}_2))
\end{aligned}
\tag{55}
$$

Because

$$
\begin{aligned}
&d_{h_3}(\phi,\theta,\omega_1,\omega_2) - d_{h_3}(\bar{\phi},\bar{\theta},\bar{\omega}_1,\bar{\omega}_2)\\
&\quad = d(\phi,\theta,\omega_1,\omega_2) - d(\bar{\phi},\bar{\theta},\bar{\omega}_1,\bar{\omega}_2)
\end{aligned}
\tag{56}
$$

it follows that $f_{h_3}(t) = f(t)$ and $f_{h_3}(t)$ converges exponentially to zero. The rest of the proof follows as the proof of lemma 1. □

Although lemma 2 is a similar result to lemma 1, a convergence result similar to Theorem 1 does not hold if $h_3 \neq 0$, because steady-state oscillations in ψ, θ, and ϕ in a vicinity of zero will occur to accommodate nonzero h_3.

The amplitude of oscillations about $\Theta = 0$ using this switching law can be bounded. Consider the situation when $\alpha_1 = \epsilon_e\alpha_{2,e}$, $\alpha_2 = \alpha_{2,e}$, the base variable motion is in steady-state, and $\psi(0) = 0$. If this is the case, then, from Eq. (21),

$$
\begin{aligned}
|\phi(t)| &= |\epsilon_e\alpha_{2,e}\beta_1(nt+\delta_1+\gamma_1)_c| \le |\epsilon_e\alpha_{2,e}\beta_1| \quad \forall\ t \ge 0,\\
|\theta(t)| &= |\alpha_{2,e}\beta_3(nt+\delta_2+\gamma_3)_c| \le |\alpha_{2,e}\beta_3| \quad \forall\ t \ge 0
\end{aligned}
\tag{57}
$$

Furthermore, for $0 \le t \le T$,

$$
\begin{aligned}
|\psi(t)| &= \int_0^t \left|\Phi(t,\tau)\left(b(\tau)+\frac{h_3}{j_{33}}\right)\mathrm{d}\tau\right| \\
&\le \int_0^t |\Phi(t,\tau)|\left|\left(b(\tau)+\frac{h_3}{j_{33}}\right)\right|\mathrm{d}\tau, \\
&\le \int_0^t |\Phi(t,\tau)|\left(|(b(\tau)|+\frac{|h_3|}{j_{33}}\right)\mathrm{d}\tau, \\
&\le \int_0^T \frac{\exp(c_2)}{j_{33}}(|\alpha_{2,e}|c_3+|h_3|)\,\mathrm{d}\tau, \\
&\le \frac{2\pi\exp(c_2)}{n j_{33}}(|\alpha_{2,e}|c_3+|h_3|)
\end{aligned}
\tag{58}
$$

in which

$$
\begin{aligned}
c_2 &= |\frac{\alpha_{2,e}}{n j_{33}}|(|\epsilon_e h_1\beta_1|+|h_2\beta_3|), \\
c_3 &= |\alpha_{2,e}\epsilon_e\beta_1\beta_4 j_{33}|+|h_1\beta_3|+|\epsilon_e h_2\beta_1|+|\epsilon_e\beta_2 j_{13}|+|\beta_4 j_{23}|
\end{aligned}
\tag{59}
$$

The value of $\alpha_{2,e}$ decreases with the value of h_3, and, furthermore, $\lim_{h_3\to 0}\alpha_{2,e}=0$. Therefore, the amplitude of the steady-state oscillation in ϕ, θ, and ψ around zero will decrease as h_3 decreases.

VI. Analysis of High-Frequency Response

We now consider the case when the base variable excitation frequency n is large and analyze the motions of Euler angles ϕ, θ and ψ when the total angular momentum is zero and when there is a nonzero total angular momentum component about the uncontrollable axis.

A. Zero Angular Momentum Case

Let $h_1=h_2=h_3=0$ and assume that $\phi(0)=\theta(0)=\psi(0)=0$. Consider the spacecraft excited by base variable motions [Eq. (21)] with constant α_1 and α_2, and let

$$\dot{\bar{\psi}} = \frac{\Delta_a\psi}{T} \tag{60}$$

in which $\Delta_a\psi$ is given by Eq. (28). Equation (60) defines an average rate of change of ψ over one steady-state cycle of period T. Substituting Eqs. (28) and (29) into Eq. (60) gives

$$\dot{\bar{\psi}} = \frac{\alpha_1\alpha_2\beta_1\beta_4}{2}(\delta_1-\delta_2+\gamma_1-\gamma_4)_c \tag{61}$$

If n is large, (22) can be approximated by

$$\beta_1\sim O\left(\frac{1}{n^2}\right),\quad \beta_2\sim O\left(\frac{1}{n^2}\right),\quad \beta_3\sim O\left(\frac{1}{n}\right),\quad \beta_4\sim O\left(\frac{1}{n}\right) \tag{62}$$

and (61) can be approximated by

$$\dot{\bar{\psi}} \sim \frac{\alpha_1\alpha_2}{n^3}(\delta_1-\delta_2+\gamma_1-\gamma_4)_c \tag{63}$$

in which γ_1 and γ_4 also depend on n. Let α_1 and α_2 be nonzero and proportional to $n^{\frac{3}{2}}$, that is,

$$\alpha_1 = n^{\frac{3}{2}}\rho_1,\quad \alpha_2 = n^{\frac{3}{2}}\rho_2 \tag{64}$$

in which $\rho_1,\rho_2\in\mathbb{R}\setminus\{0\}$. The steady-state values of ϕ and θ from Eq. (21) when n is large are approximated by

$$\bar{\phi}(t)\sim\frac{\rho_1}{\sqrt{n}}\cos(nt+\delta_1+\gamma_1)_c,\quad \bar{\theta}(t)\sim\frac{\rho_2}{\sqrt{n}}\cos(nt+\delta_2+\gamma_3)_c \tag{65}$$

As n approaches infinity, for any t, it is clear from Eq. (65) that

$$\lim_{n\to\infty}\bar{\phi}(t)=0,\quad \lim_{n\to\infty}\bar{\theta}(t)=0 \tag{66}$$

Note that γ_1 and γ_4 have finite limits, $\bar{\gamma}_1$ and $\bar{\gamma}_4$, respectively, as n increases. Then,

$$\lim_{n\to\infty}\dot{\bar{\psi}} = \rho_1\rho_2(\delta_1-\delta_2+\bar{\gamma}_1-\bar{\gamma}_4)_c \tag{67}$$

Hence, as frequency increases, attitude trajectories of an underactuated spacecraft with zero total angular momentum can approach arbitrary close attitude trajectories of a spacecraft that has a nonzero total angular momentum component and rotates at a constant angular velocity about the uncontrollable axis. Note that, as frequency n increases, the amplitude of the spacecraft angular velocity and RW speed oscillation increase as $\sqrt{n}$.

B. Nonzero Angular Momentum Case

The same approach as in Sec. VI.A is used to analyze a spacecraft that has nonzero total angular momentum about its uncontrollable axis. Assume that $\phi(0)=\theta(0)=\psi(0)=0$, $h_1,h_2\in\mathbb{R}$, and $h_3\neq 0$. Define,

$$\dot{\bar{\psi}}_{h_3} = \frac{\Delta\psi_{h_3}}{T} \tag{68}$$

in which $\Delta_{a,h_3}\psi$ is given by Eq. (46). Let α_1 and α_2 be defined as in Eq. (64). If the frequency is increased to infinity, then

$$
\begin{aligned}
&\lim_{n\to\infty}\bar{\phi}(t)=0, \\
&\lim_{n\to\infty}\bar{\theta}(t)=0, \\
&\lim_{n\to\infty}\dot{\bar{\psi}} = \frac{h_3}{j_{33}}+\rho_1\rho_2(\delta_1-\delta_2+\bar{\gamma}_1-\bar{\gamma}_4)_c
\end{aligned}
\tag{69}
$$

in which $\bar{\gamma}_1$ and $\bar{\gamma}_4$ denote finite limits of γ_1 and γ_4 as n increases. Choosing ρ_1 and ρ_2 so that

$$\rho_1\rho_2 = -\frac{h_3}{j_{33}(\delta_1-\delta_2+\bar{\gamma}_1-\bar{\gamma}_4)_c} \tag{70}$$

results in

$$\lim_{n\to\infty}\dot{\bar{\psi}} = 0 \tag{71}$$

As n increases, attitude trajectories of the underactuated spacecraft with a nonzero total angular momentum component about the uncontrollable axis can approach arbitrarily close to a fixed inertial pointing attitude. Similarly to the zero total angular momentum case, as n increases, the amplitude of the spacecraft angular velocity and RW speed oscillation increase as $\sqrt{n}$.

Table 1 Controller and algorithm parameters

Parameter	Value
n	$0.03\ \mathrm{s}^{-1}$
k_{11}, k_{12}	9×10^{-4}, 0.0180
k_{21}, k_{22}	9×10^{-4}, 0.0180
δ_1, δ_2	$\frac{\pi}{4}, -\frac{\pi}{4}$
ξ_1, ξ_2, ξ_3	1×10^{-4}, 1.5, 2.5×10^{-5}
μ_1, μ_2	0.5, 1×10^{-8}

Remark 3: The conclusions in this section may appear to be counterintuitive at first glance given the angular momentum conservation. In [28], similar results were derived using averaging theory for a different system, a cylinder rotating about a fixed axis with three movable links.

VII. Simulation Results

For the simulations, we consider a spacecraft bus with the principal moments of inertia of 430, 1210, and 1300 $\mathrm{kg \cdot m^2}$. The two reaction wheels are assumed to be symmetric and thin and are mounted such that the COM of the spacecraft bus and total spacecraft assembly coincide. The inertias of the two functioning RWs about their spin axes are given by $J_{s1} = J_{s2} = 0.043\ \mathrm{kg \cdot m^2}$. The matrices $\bar{J}$ and $\bar{W}$ will be different between simulations as necessary to demonstrate that our approach can handle different spacecraft scenarios. In the first simulation, the spacecraft has zero total angular momentum. The second simulation involves a spacecraft with total angular momentum satisfying proposition 1 (i.e., $h_3 = 0$). In the third simulation, $h_3 \neq 0$. All simulations are performed on the full

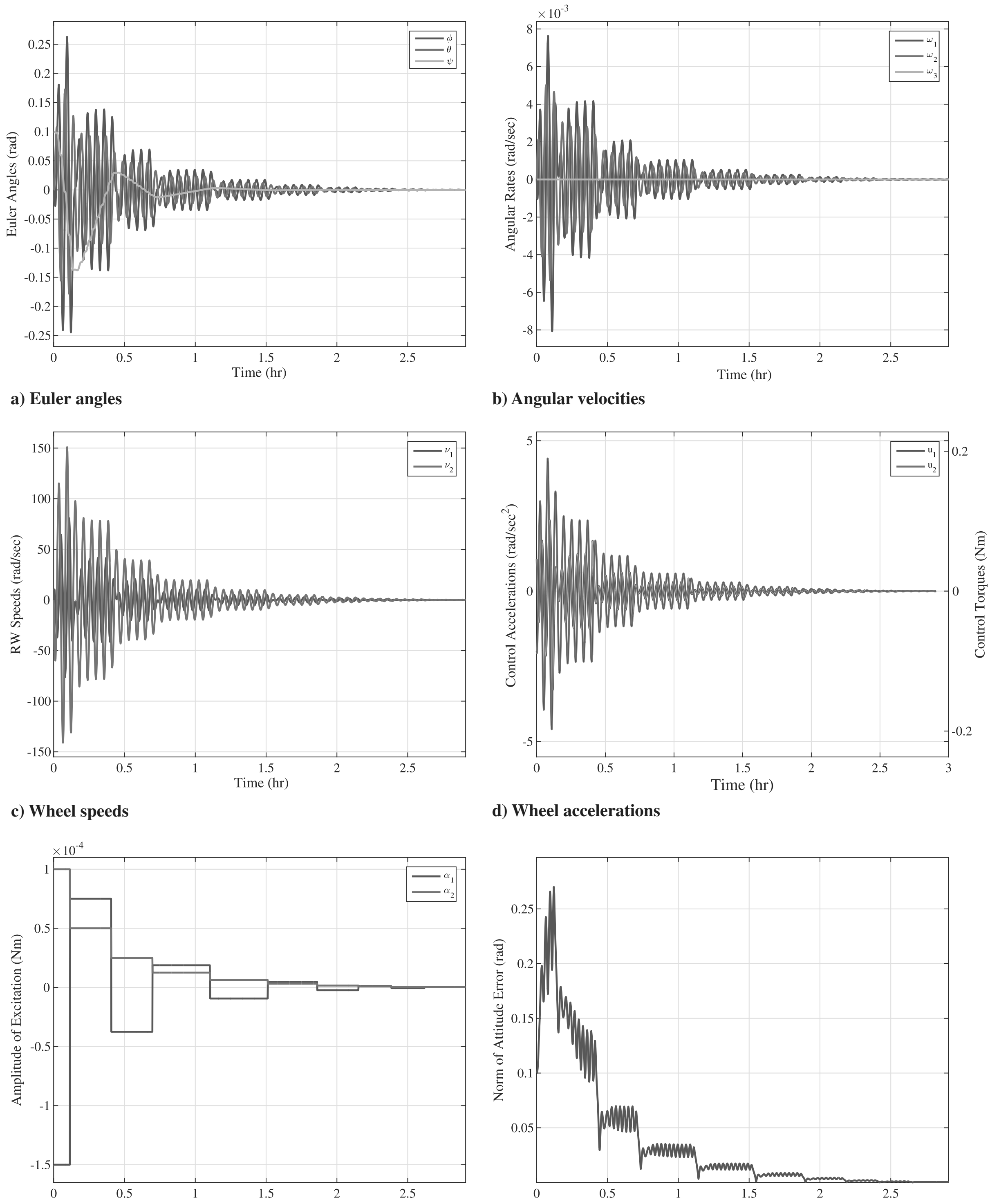

a) Euler angles

b) Angular velocities

c) Wheel speeds

d) Wheel accelerations

e) Excitation magnitude

f) 2-norm of attitude error

Fig. 4 Response of the spacecraft assembly defined in Sec. VII.A using Algorithm 1 when $H = 0$.

nonlinear model and demonstrate successful convergence to the desired pointing equilibrium in the case when $h_3 = 0$ and controlled oscillation about the desired pointing configuration when $h_3 \neq 0$. The parameters for the controller and switching schemes, outlined by Algorithms 1 and 2, are given in Table 1.

A. Simulation 1

Consider the case when the two RWs are aligned with the first two principal axes of the spacecraft bus. Then

$$\bar{J} = \begin{bmatrix} 430.043 & 0 & 0 \\ 0 & 1210.043 & 0 \\ 0 & 0 & 1300 \end{bmatrix}, \quad \bar{W} = \begin{bmatrix} 0.043 & 0 \\ 0 & 0.043 \\ 0 & 0 \end{bmatrix} \tag{72}$$

The initial conditions of the spacecraft are $\phi(0) = \theta(0) = 0$ rad, $\psi(0) = 0.1$ rad, $\omega_1(0) = \omega_2(0) = \omega_3(0) = 0$ rad/s, and $\nu_1(0) = \nu_2(0) = 0$ rad/s. The total angular momentum is hence zero [i.e., $H = [0 \quad 0 \quad 0]^T$ $(\mathrm{kg \cdot m^2})/\mathrm{s}$] and satisfies proposition 1. The simulation shows that, by using Algorithm 1, the spacecraft

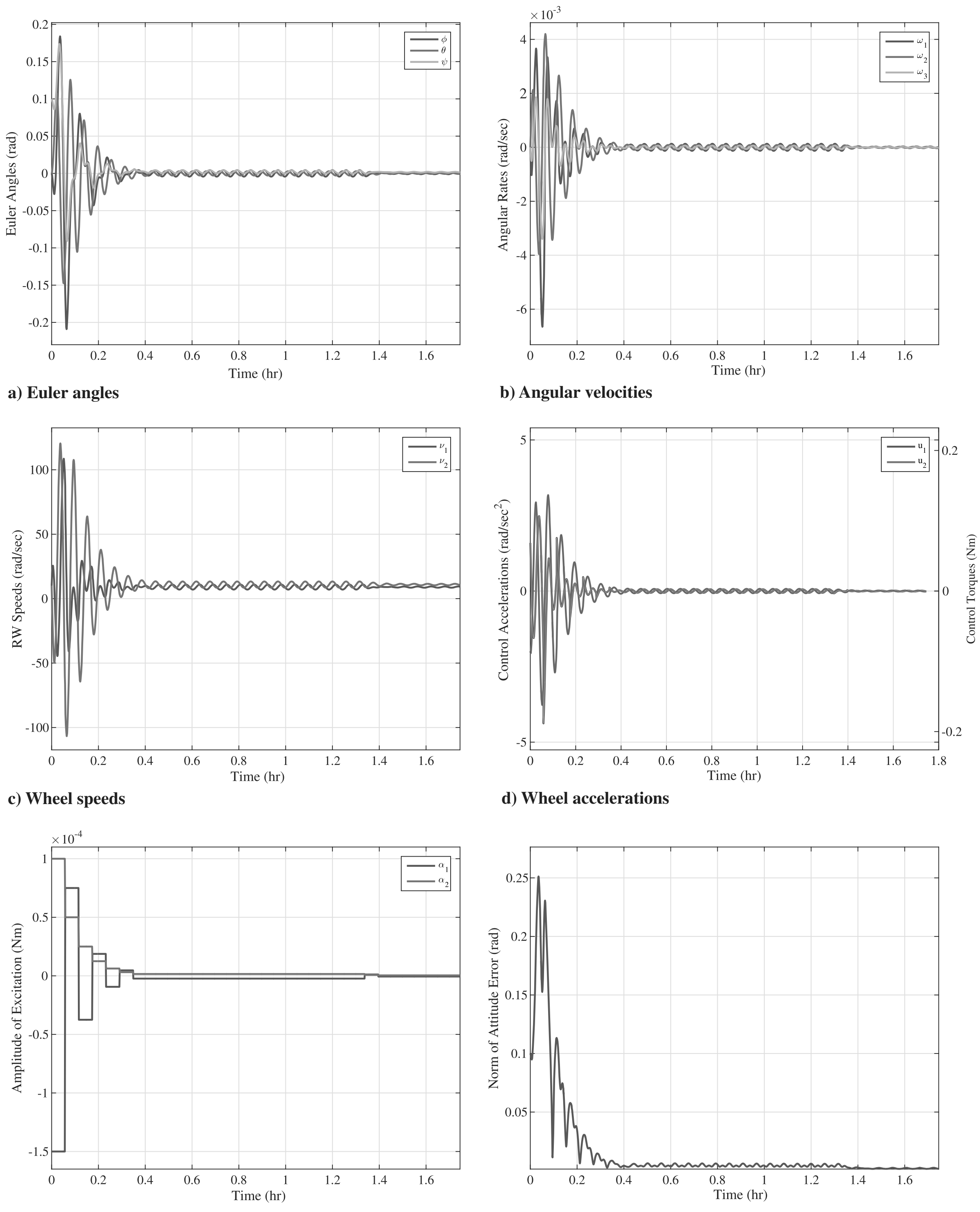

a) Euler angles

b) Angular velocities

c) Wheel speeds

d) Wheel accelerations

e) Excitation magnitude

f) 2-norm of attitude error

Fig. 5 Response of the spacecraft assembly defined in Sec. VII.B using Algorithm 1 when $h_3 = 0$.

successfully converges to the desired pointing orientation. See Fig. 4. Note from Figs. 4a and 4e that, when α_1 changes sign (which is dictated by ϵ), the direction of $\Delta\psi$ also changes.

Remark 4: It should be noted that even though the convergence time is exponential, the convergence time for this simulation is over two hours. The convergence time can be improved by tuning the parameters in Table 1, specifically ξ_1 and ξ_2 (which govern the initial amplitude of the excitation), μ_1 (which controls the decay of excitation), and n (which defines when the control parameters are switched).

B. Simulation 2

Now consider the case when the RWs are not aligned with the first two principal axes of the spacecraft bus. After an appropriate coordinate transformation, the matrices $\bar{J}$ and $\bar{W}$ are

$$\bar{J} = \begin{bmatrix} 865 & 0 & -0.435 \\ 0 & 1210.043 & 0 \\ -0.435 & 0 & 865.043 \end{bmatrix}, \quad \bar{W} = \begin{bmatrix} 0.043 & 0 \\ 0 & 0.043 \\ 0 & 0 \end{bmatrix} \tag{73}$$

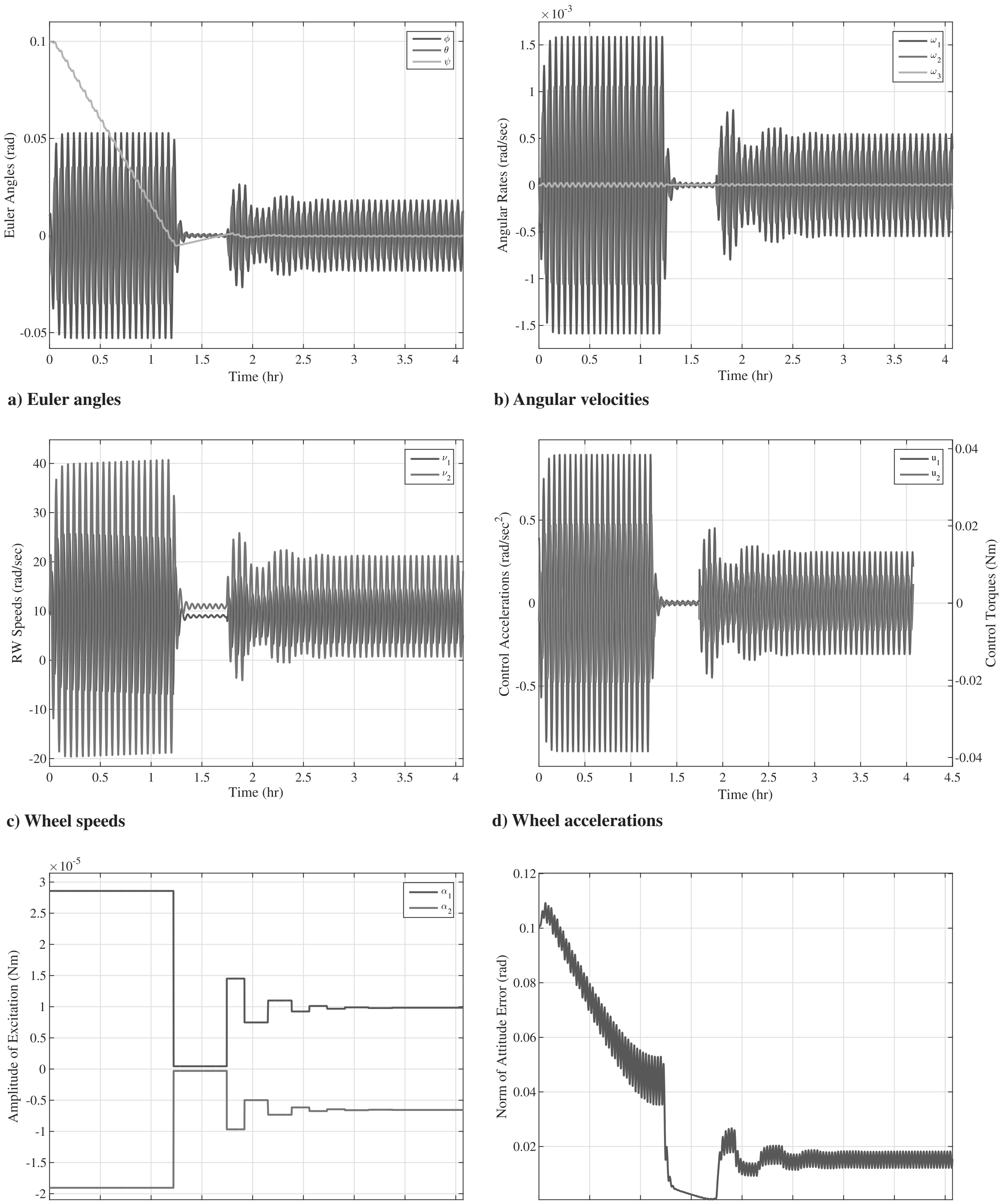

a) Euler angles

b) Angular velocities

c) Wheel speeds

d) Wheel accelerations

e) Excitation magnitude

f) 2-norm of attitude error

Fig. 6 Response of the spacecraft assembly defined in Sec. VII.C using Algorithm 2 when $h_3 \neq 0$.

The initial conditions for the spacecraft are the same as for simulation 1 with the exception that $\nu_1(0) = \nu_2(0) = 10$ rad/s, yielding $H = [0.3849 \quad 0.4708 \quad 0]^T$ (kg $\cdot$ m^2)/s, which satisfies proposition 1. The results are shown in Fig. 5. As is demonstrated, even though the RWs are not aligned with the principal axes, Algorithm 1 is still able to guide the system to the pointing equilibrium. Note that the RW speeds are not zero in steady-state and absorb the nonzero total angular momentum of the spacecraft. The stabilization of this system takes a shorter amount of time compared with simulation 1. In this case, the added angular momentum and the nondiagonal shape of $\bar{J}$ induce nonlinear terms that improve the convergence time, but this may not be always the case.

C. Simulation 3

Consider now the case when the RWs spin about the first two principal axes of the spacecraft bus. In this case, the matrices $\bar{J}$ and $\bar{W}$ are the same as in simulation 1. Let $\phi(0) = 0.01$ rad, $\theta(0) = 0$ rad, $\psi(0) = 0.1$ rad, $\omega_1(0) = \omega_2(0) = \omega_3(0) = 0$ rad/s, and $\nu_1(0) = \nu_2(0) = 10$ rad/s. In this case, $H = [0.3849 \; 0.4708 \; 0.0043]^T$ kg$\cdot$m^2/s, and does not satisfy proposition 1. Figure 6 demonstrates the response of the spacecraft using Algorithm 2. Note that the attitude error in Fig. 6f reaches near zero but then increases. This is due to the fact that simultaneous convergence of all three Euler angles to zero is impossible because the spacecraft is underactuated and has a nonzero total angular momentum component about the uncontrollable axis (proposition 1). However, Fig. 6a demonstrates that, by using Algorithm 2, controlled and bounded oscillations in a vicinity of $\Theta = 0$ can be performed.

Remark 5: As mentioned in the introduction, the treatment of an underactuated spacecraft with nonzero total angular momentum has been limited. Even in the case when total angular momentum is taken into account, some proposed control schemes can send a spacecraft into an uncontrolled drift (see [21]). In [12,14], it was shown that a Lyapunov-based controller designed for zero total angular momentum could perform oscillations about the desired pointing configuration when there was a nonzero component of total angular momentum about the uncontrollable axis. However, the Lyapunov functions used for controller synthesis in each method become undefined at certain orientations near the desired attitude, and thus singularity avoidance must be performed. This method, in contrast, does not have such singularity issues. Another benefit to the switching law presented in our paper is that the total angular momentum is taken into account when designing the controller, which could improve overall performance.

VIII. Conclusions

This paper presented a switching feedback law to locally control the attitude of an underactuated spacecraft with two reaction wheels (RWs) to an inertial pointing configuration. The feedback law exploits the decomposition of the system states into base variables that are directly controllable and fiber variables that are not directly controllable. By stabilizing the base variables to periodic motions, a change in the fiber variables can be induced, which is regulated by changing parameters at discrete time instants. The switching scheme was shown to stabilize an underactuated spacecraft to the desired pointing configuration when the component of the total, inertial angular momentum vector along the uncontrollable axis is zero. If this is not the case, controlled oscillations in a neighborhood around the desired pointing configuration were achieved with a modified switching scheme. Simulation results were reported that demonstrate the proposed control scheme can successfully perform the desired spacecraft attitude maneuvers. Additional analysis results of the spacecraft response properties were presented to characterize trajectory limits as the excitation frequency of the base variables increases.

References

[1] Crouch, P., "Spacecraft Attitude Control and Stabilization: Applications of Geometric Control Theory to Rigid Body Models," *Transactions on Automatic Control*, Vol. 29, No. 4, 1984, pp. 321–331. doi:10.1109/TAC.1984.1103519

[2] Cowen, R., "The Wheels Come Off Kepler," *Nature*, Vol. 497, May 2013, pp. 417–418, http://www.nature.com/news/the-wheels-come-off-kepler-1.13032 [retrieved 18 Oct. 2013]. doi:10.1038/497417a

[3] Moos, H. W., "Overview of the Far Ultraviolet Spectroscopic Explorer Mission," *The Astrophysical Journal Letters*, Vol. 538, No. 1, July 2000, pp. L1–L6. doi:10.1086/312795

[4] de Selding, P. B., "Japan's Asteroid Sample-Return Mission Has Problems," *Space.com*, Oct. 2005, http://www.space.com/1642-japan-asteroid-sample-return-mission-problems.html [retrieved 29 July 2015].

[5] Krishnan, H., McClamroch, H., and Reyhanoglu, M., "Attitude Stabilization of a Rigid Spacecraft Using Two Momentum Wheel Actuators," *Journal of Guidance, Control, and Dynamics*, Vol. 18, No. 2, 1995, pp. 256–263. doi:10.2514/3.21378

[6] Brockett, R. W., "Asymptotic Stability and Feedback Stabilization," *Differential Geometric Control Theory*, edited by Brockett, R. W., Millman, R. S., and Sussmann, H. J., Birkhauser, Boston, MA, 1983, pp. 181–191.

[7] Byrnes, C. I., and Isidori, A., "On the Attitude Stabilization of Rigid Spacecraft," *Automatica*, Vol. 27, No. 1, 1991, pp. 87–95. doi:10.1016/0005-1098(91)90008-P

[8] Zabczyk, J., "Some Comments on Stabilizability," *Applied Mathematics and Optimization*, Springer–Verlag, New York, 1989, pp. 1–9.

[9] Gurvits, L., and Li, Z., "Smooth Time-Periodic Feedback Solutions for Nonholonomic Motion Planning," *Progress in Nonholonomic Motion Planning*, Springer, New York, 1993, pp. 53–108. doi:10.1007/978-1-4615-3176-0_3

[10] Ge, X., and Chen, L., "Optimal Reorientation of Underactuated Spacecraft Using Genetic Algorithm with Wavelet Approximation," *Acta Mechanica Sinica*, Vol. 25, No. 4, 2009, pp. 547–553. doi:10.1007/s10409-009-0246-6

[11] Gui, H., Jin, L., and Xu, S., "Attitude Maneuver Control of a Two-Wheeled Spacecraft with Bounded Wheel Speeds," *Acta Astronautica*, Vol. 88, 2013, pp. 98–107. doi:10.1016/j.actaastro.2013.03.006

[12] Horri, N. M., and Hodgart, S., "Attitude Stabilization of an Underactuated Satellite Using Two Wheels," *Proceedings of the Aerospace Conference*, Vol. 6, IEEE Publ., Piscataway, NJ, Nov. 2003, pp. 2629–2635. doi:10.1109/AERO.2003.1235188

[13] Horri, N. M., and Palmer, P., "Practical Implementation of Attitude-Control Algorithms for an Underactuated Satellite," *Journal of Guidance, Control, and Dynamics*, Vol. 35, No. 1, 2012, pp. 40–45. doi:10.2514/1.54075

[14] Urakubo, T., Tsuchiya, K., and Tsujita, K., "Attitude Control of a Spacecraft with Two Reaction Wheels," *Journal of Vibration and Control*, Vol. 10, No. 9, 2004, pp. 1291–1311. doi:10.1177/1077546304042042

[15] Liu, W., "Averaging Theorems for Highly Oscillatory Differential Equations and the Approximation of General Paths by Admissible Trajectories for Nonholonomic Systems," Ph.D. Dissertation, Department of Mathematics and Rutgers, New Brunswick, NJ, 1992.

[16] Leonard, N. E., and Krishnaprasad, P. S., "Averaging for Attitude Control and Motion Planning," *Proceedings of the 32nd Conference on Decision and Control*, Vol. 4, IEEE Publ., Piscataway, NJ, Dec. 1993, pp. 3098–3104. doi:10.1109/CDC.1993.325773

[17] Leonard, N. E., and Krishnaprasad, P. S., "Motion Control of Drift-Free, Left-Invariant Systems on Lie Groups," *Transactions on Automatic Control*, Vol. 40, No. 9, Sept. 1995, pp. 1539–1554. doi:10.1109/9.412625

[18] Yamada, K., Yoshiwa, S., and Yamaguchi, I., "Feedback Attitude Control of a Spacecraft by Two Reaction Wheels," *Proceedings of the International Symposium on Space Technology and Science*, Vol. 21, Agne Shofu Publishing Inc., Tokyo, 1998, pp. 550–555.

[19] Boyer, F., and Alamir, M., "Further Results on the Controllability of a Two-Wheeled Satellite," *Journal of Guidance, Control, and Dynamics*, Vol. 30, No. 2, March–April 2007, pp. 611–619. doi:10.2514/1.21505

[20] Kim, S., and Kim, Y., "Spin-Axis Stabilization of a Rigid Spacecraft Using Two Reaction Wheels," *Journal of Guidance, Control, and Dynamics*, Vol. 24, No. 5, 2001, pp. 1046–1049. doi:10.2514/2.4818

[21] Katsuyama, Y., Sekiguchi, K., and Sampei, M., "Spacecraft Attitude Control by 2 Wheels with Initial Angular Momentum," *Proceedings of*

the SICE Annual Conference, IEEE Publ., Piscataway, NJ, 2013, pp. 1890–1895.

[22] Flynn, M., Leve, F., Petersen, C., and Kolmanovsky, I., "Linear Control of Underactuated Spacecraft with Two Reaction Wheels Made Feasible by Solar Radiation Pressure," *Proceedings of the American Control Conference*, IEEE Publ., Piscataway, NJ, 2015, pp. 3193–3198. doi:10.1109/ACC.2015.7171824

[23] Petersen, C., Leve, F., Flynn, M., and Kolmanovsky, I., "Recovering Linear Controllability of an Underactuated Spacecraft by Exploiting Solar Radiation Pressure," *Journal of Guidance, Control, and Dynamics*, Vol. 39, No. 4, 2016, pp. 826–837. doi:10.2514/1.G001446

[24] Kolmanovsky, I., and McClamroch, N. H., "Hybrid Feedback Laws for a Class of Cascade Nonlinear Control Systems," *Transactions on Automatic Control*, Vol. 41, No. 9, 1996, pp. 1271–1282. doi:10.1109/9.536497

[25] Rui, C., Kolmanovsky, I., and McClamroch, H., "Hybrid Control for Stabilization of a Class of Cascade Nonlinear Systems," *Proceedings of the American Control Conference*, Vol. 5, IEEE Publ., Piscataway, NJ, June 1997, pp. 2800–2804. doi:10.1109/ACC.1997.611966

[26] Petersen, C., Leve, F., and Kolmanovsky, I., "Hybrid Switching Attitude Control of Underactuated Spacecraft Subject to Solar Radiation Pressure," *Proceedings of the Spaceflight Mechanics Meeting*, AIAA Paper 2015-0327, Williamsburg, VA, 2015.

[27] Hughes, P., "Rotational Kinematics," *Spacecraft Attitude Dynamics*, edited by Hughes, P., Dover Publ., Mineda, NY, 2004, pp. 18–28.

[28] Kolmanovsky, I., and McClamroch, N. H., "Controllability and Motion Planning for Noncatastatic Nonholonomic Control Systems," *Mathematical and Computer Modeling*, Vol. 24, No. 1, 1996, pp. 31–42. doi:10.1016/0895-7177(96)00078-7